Vol. 506: 145–161, 2014
doi: 10.3354/meps10816

MARINE ECOLOGY PROGRESS SERIES
Mar Ecol Prog Ser

Published June 23

High-resolution ecological niche modelling of the cold-water coral *Lophelia pertusa* in the Gulf of Mexico

Samuel E. Georgian[1,*], William Shedd[2], Erik E. Cordes[1]

[1]Department of Biology, Temple University, 1900 N 12th Street, Philadelphia, Pennsylvania 19122, USA
[2]Bureau of Ocean Energy Management, US Department of the Interior, 1201 Elmwood Park Boulevard, New Orleans, Louisiana 70123, USA

ABSTRACT: The niche of many deep-sea species remains poorly resolved despite decades of seafloor exploration. Without better information on the distribution and habitat preference of key species, a complete understanding of the ecology of deep-sea communities will remain unattainable. It is increasingly apparent that cold-water corals are among the dominant foundation species in the deep sea, providing both structurally complex habitat and significant ecosystem services. In this study, the niche and distribution of the cold-water coral *Lophelia pertusa* in the Gulf of Mexico was evaluated using the maximum entropy (Maxent) approach. Ecological niche models were constructed for a broad region of the northern Gulf of Mexico using data gridded at a spatial resolution of 25 m, including bathymetry, substrate type, export productivity, and aragonite saturation state at depth. Fine-scale models were constructed at a resolution of 5 m using only remotely sensed bathymetric and surface reflectivity data. The broad-scale model performed well, with an area under the curve (AUC) of 0.981. All fine-scale models performed well when verified using training data (average AUC of 0.963) and when validated using independent occurrence data from a new geographic region (average AUC of 0.937). The distribution of *L. pertusa* in the Gulf of Mexico was found to be controlled primarily by depth, local topography, and availability of hard substrate. While these factors have long been associated with the success of cold-water corals, their relative importance has never been quantified in the Gulf of Mexico, making it historically difficult to precisely delineate *L. pertusa*'s niche and predict its distribution in unexplored regions. Given these results, we suggest that future expeditions combine remotely sensed data with niche modelling techniques to increase the efficiency of deep-sea exploration.

KEY WORDS: Bathymetry · Cold-water corals · Gulf of Mexico · *Lophelia pertusa* · Niche modelling · Maxent

INTRODUCTION

Understanding the environmental and geographic distribution of species is an ongoing challenge in deep-sea ecology. Distribution patterns in the deep sea are generally poorly resolved, in part because of the difficulty and expense of surveying deep-water regions and the vast area of unexplored seafloor (e.g. Gage 2004). It has been estimated that only 0.0001% of the deep sea has been visually surveyed (Gjerde 2006), and much of this past work has focused on a few relatively well studied areas (e.g. the northeastern Atlantic). A better understanding of species' biogeographic distributions is fundamental for designing and implementing management plans, shaping future research efforts, and assessing anthropogenic impacts. Given the recent increase in the rate and scale of anthropogenic disturbance to the deep sea

*Corresponding author: georgian@temple.edu

(Glover & Smith 2003, Guinotte & Fabry 2008, Montagna et al. 2013), it is imperative to more fully characterize the distribution and niche of deep-sea species before these ecosystems are irrevocably altered or lost.

Cold-water corals support biodiversity hotspots in the deep sea by creating structurally complex habitats and providing ecosystem services such as nutrient cycling and carbon sequestration (Buhl-Mortensen et al. 2010). *Lophelia pertusa* (Linnaeus 1758) is one of the most abundant and widespread cold-water corals (Roberts et al. 2009). It forms extensive reef structures that cover areas on the order of kilometers squared and over 100 m high (De Mol et al. 2002, Wheeler et al. 2007) and serve as important carbon sinks in the deep sea (van Weering et al. 2003). Over 1300 species were found to associate with *L. pertusa* reefs in the North Atlantic (Roberts et al. 2006), including several commercially important fish (Costello et al. 2005). Extant cold-water coral mounds have been shown to demonstrate continuous growth for the past 50000 years or longer (Schröder-Ritzrau et al. 2005), suggesting that the distribution of *L. pertusa* may be structured primarily by environmental factors that are relatively stable over long time periods. However, the factors responsible for controlling its distribution in the Gulf of Mexico are only partially understood (Schroeder et al. 2005, Cordes et al. 2008, Davies et al. 2010).

Previous work has shown that cold-water corals typically occur on elevated and irregular seafloor features where the current regime and topography combine to generate locally accelerated, turbulent flows that increase food availability, larval dispersal, and sediment and waste removal (Thiem et al. 2006, Dorschel et al. 2007, White et al. 2007, Mienis et al. 2012). The availability of hard substrata is thought to be a requirement for larval recruitment (e.g. Freiwald et al. 1999). However, settlement also occurs on mixed bottoms, small substrata (including shells, cobbles, or boulders), and man-made objects (Wilson 1979, Gass & Roberts 2006, Larcom et al. 2013), and the extent to which substrate may structure spatial distributions remains unclear. The success of cold-water corals is also influenced by the aragonite or calcite saturation state, with numerous field studies reporting that most cold-water corals persist and grow at higher saturation states (Guinotte et al. 2006, Lunden et al. 2013) and experimental results that demonstrate an energetic cost associated with calcification at low saturation states (e.g. Turley et al. 2007, Maier et al. 2009). Finally, cold-water corals are heterotrophic filter feeders that are reliant on the transfer of energy from surface primary production (Roberts et al. 2009), of which only 1 to 3% reaches the deep sea (Deuser 1986). Therefore, cold-water corals are expected to occur in regions that receive a high export of surface productivity (e.g. Tittensor et al. 2009).

Ecological niche models are an emerging tool being used to characterize the distribution of both terrestrial and marine organisms by statistically coupling occurrence records with environmental parameters. This approach has recently gained traction in the deep sea, where extensive direct observations are logistically difficult, and occurrence data are often sparse. *L. pertusa* has been modelled globally at a scale of 30 arc seconds (approximately 1 km), with depth, temperature, and aragonite saturation state found to be the most important drivers of its distribution (Davies & Guinotte 2011). Tittensor et al. (2009) similarly produced a global model of cold-water scleractinian corals on seamounts using a grid size of approximately 1° and found that occurrence was positively linked with high aragonite saturation states and elevated dissolved oxygen concentrations. Other studies have modelled *L. pertusa*'s niche at regional scales using finer spatial resolutions ranging from 30 to 750 m (Guinan et al. 2009, Howell et al. 2011, Rengstorf et al. 2013, Ross & Howell 2013). In addition, Dolan et al. (2008) used a multibeam system mounted on a remotely operated vehicle (ROV) to model suitable habitat at a resolution of 0.5 m; however, they did not differentiate between occurrences of *L. pertusa* and *Madrepora oculata*, which are thought to fill different niches (Orejas et al. 2009). Notably, none of these modelling studies included the Gulf of Mexico, which is geologically unique (Bryant et al. 1990) and contains genetically isolated *L. pertusa* populations (Morrison et al. 2011). Therefore, it is possible that *L. pertusa* occupies a different niche in the Gulf of Mexico than in other biogeographic regions, as has been shown in other species (see review by Pearman et al. 2008).

Niche models can be especially vital for conservation efforts when the rate of anthropogenic disturbance greatly outpaces our ability to survey benthic environments and identify sensitive coral habitats, as appears to be the case in the deep Gulf of Mexico (White et al. 2012). There is an immediate need to better establish the niche of *L. pertusa* in the Gulf of Mexico and to develop a better approach for locating novel coral sites. The aim of this study was to use ecological niche modelling to quantify the aspects of *L. pertusa*'s niche that relate to the availability of hard substrate, aragonite saturation state, export pro-

ductivity, and seafloor topography. In addition, we sought to map potentially suitable habitat in the northern Gulf of Mexico at 2 spatial scales to inform conservation and management decisions and to facilitate the discovery of new *L. pertusa* reefs in the region.

MATERIALS AND METHODS

Presence data

We classified study sites according to their location within the U.S. Bureau of Ocean Energy Management (BOEM) lease blocks in the Viosca Knoll (VK), Garden Banks (GB), Green Canyon (GC), and Mississippi Canyon (MC) protraction areas (see Table 1). Video data collected during ROV and human-operated vehicle (HOV) dives spanning from 2005 to 2013 — all cruises associated with the *Lophelia* I and II projects, funded by the BOEM and NOAA Office of Exploration and Research (OER), and cruise NA028 of the Ecosystem Impacts of Oil and Gas Inputs to the Gulf (ECOGIG) project — were reviewed to extract the presence of living *Lophelia pertusa* colonies. These occurrences were linked to ultra-short baseline navigational data (slant error of 1%) to yield a set of georeferenced locations. Live *L. pertusa* colonies are highly visible and easily distinguishable from other species, making the probability of detection extremely high within the field of view of surveyed areas. Additional occurrences were obtained from data logs recorded during the cruises listed above, Schroeder et al. (2005), and the Smithsonian National Museum of Natural History (NMNH) database. Only occurrence records obtained from direct observation were included from the NMNH database to avoid potential inaccuracies in the recorded location of samples collected by trawling or unknown methods and to avoid the use of occurrences of dead coral skeleton of unknown age. Duplicate occurrences within the same grid cell were removed prior to analysis.

Environmental data

Analysis scale

Modelling the ecological niche is highly dependent on choosing the appropriate scale for analysis, regarding both the grain and extent of environmental variables (Wheatley & Johnson 2009). This is especially true with terrain variables, which are inherently scale dependent. Previous work with *Lophelia pertusa* has demonstrated the importance of seafloor features including fine-scale sediment waves (Dolan et al. 2008), carbonate mounds (Guinan et al. 2009), seamounts (Tittensor et al. 2009), and continental slopes (Davies & Guinotte 2011). Therefore, we used a multiscale approach to model *L. pertusa*'s distribution at a fine-scale resolution (5 m) at 7 sites covering a total of 189 km^2 and at a broad-scale resolution (25 m) covering 67 000 km^2 in the northern Gulf of Mexico. Within our study area, *L. pertusa* commonly grows in small, isolated thickets (<2 m across) that are likely to be influenced by local features best characterized on a fine scale. However, at numerous locations, it grows in large reef patches tens or hundreds of meters across that are more likely to be influenced by broad-scale factors. Therefore, this combination of scales is expected to capture the full range of environmental variation likely to be controlling *L. pertusa*'s distribution in the Gulf of Mexico. In addition, the coarser resolution of the broad-scale model allowed for the inclusion of environmental variables that did not exist at a high enough resolution to inform fine-scale models.

Broad-scale model

Variables were selected *a priori* based on environmental factors believed or known from previous work to influence cold-water coral growth and survival. Bathymetric data were obtained from the Texas Sea Grant College Program (publicly available at http://gcoos.tamu.edu/products/topography) and gridded at their native resolution of 25 m using the World Geodetic System 1984 geographic coordinate system. Slope, aspect, roughness, and 3 types of curvature were calculated from this bathymetry layer using DEM Surface Tools (v2.1.292; Jenness 2013). Slope was measured in degrees using the 4-cell method (Fleming & Hoffer 1979), which has been shown to marginally outperform Horn's method, the default in ArcGIS (Horn 1981, see Jones 1998). Benthic environments with steeper slopes generally have locally accelerated currents and, as a result, considerably different facies and community types (Mohn & Beckmann 2002). The direction of the steepest slope, referred to as aspect, has a strong effect on the current regime in areas with a strong unidirectional current and has been shown to partially determine the distribution of filter feeders including *Lophelia pertusa* (Guinan et al. 2009). Aspect has an inherent

circularity when calculated in radians; therefore, it was cosine transformed to create an index of northness and sine transformed to create an index of eastness. Roughness is a measure of topographical complexity, with areas with greater complexity often exhibiting higher diversity levels (e.g. Kostylev et al. 2005). We estimated roughness as the 'surface ratio' in DEM Surface Tools, calculated as the ratio of surface area (as defined by Jenness 2004) to planimetric area. We calculated 3 types of curvature following Jenness (2013) to quantify the shape of the seafloor and how water is expected to flow over surfaces (Evans 1980, Moore et al. 1991, Wood 1996, Porres de la Haza & Pardo Pascual 2002). General curvature assigns more positive values to more convex seafloor surfaces and more negative values to more concave surfaces. Cross-sectional curvature values indicate that water is expected to diverge at positive values and converge at negative values. Positive longitudinal curvature values indicate that water is expected to decelerate, and negative values indicate that water should accelerate. Finally, we calculated the topographic position index (TPI; Weiss 2001) using Land Facet Corridor Designer (v1.2.884; Jenness et al. 2013). TPI quantifies the relative elevation of points considering their surrounding features and is thought to be important for filter feeders that may have a preference for elevated topography that is more exposed to currents (e.g. Wilson et al. 2007). To assess the potential role of both large and small seafloor features, we calculated TPI at the finest scale allowed by the resolution of the bathymetry data and at a broader scale determined empirically through a model selection process (see 'Model tuning').

Seafloor locations containing hard substrata were available as a single polygon layer from BOEM and were converted to a 25 m resolution binomial grid (1 = hard bottom, 0 = soft bottom). These data were generated from 3-dimensional seismic data originally acquired by the oil industry and managed by BOEM. The acoustic horizon of the seafloor was mapped using both automatic interpretation software (GeoFrame, Schlumberger) and manual interpretation of high-amplitude sites. These relatively low resolution seismic data have a frequency at the seafloor of approximately 50 to 60 Hz and a vertical resolution of 8 to 12 m. The horizontal samples vary from survey to survey but are typically 15 to 25 m. 'High positive' anomalies are acoustically faster than both seawater and soft bottoms, resulting in strong responses on the amplitude maps. In the Gulf of Mexico, a high positive response is often exhibited because of the presence of acoustically fast authigenic carbonates formed by microbial oxidation of hydrocarbons. These rocky, calcium carbonate substrates are suitable habitats for corals and other sessile invertebrates, provided that bottom currents are adequate to prevent sedimentation of the rock surface (e.g. Schroeder 2002).

Aragonite saturation states were calculated from total alkalinity and pH values measured in water samples obtained at depth from a 2010 cruise on the R/V 'Ronald H. Brown' (Lunden et al. 2013) and calculated from carbonate data collected during a 2007 Gulf of Mexico and East Coast Carbon cruise (Wang et al. 2013). Within the study region, aragonite saturation states averaged 1.52 and ranged from 0.98 to 4.94. To eliminate gaps between points, these data were interpolated to a slightly higher spatial resolution using the inverse distance weighting function in ArcGIS 10.1 with default parameters (power = 2, search radius = variable, number of points = 12). Export productivity (mg C m^{-2} d^{-1}) was modelled as particulate organic carbon (POC) flux to the seafloor from surface net primary productivity (NPP) using the negative depth (Z) decay exponential function: POC flux = $3.523 \times NPP \times Z^{-0.734}$ (Pace et al. 1987). NPP (g m^{-2} d^{-1}) was modelled using the Eppley Vertically Generalized Production Model (Eppley 1972, Behrenfeld & Falkowski 1997, see Carr et al. 2006) using surface chl *a*, photosynthetically available radiation, and sea surface temperature data from the moderate resolution imaging spectroradiometer. Data layers were downloaded as the 2002–2012 average at a spatial resolution of 0.416° using Marine Geospatial Ecology Tools for ArcGIS 10.2 (Roberts et al. 2010). Euphotic depth was estimated using the Case I Morel & Berthon (1989) model. Export productivity within the study area averaged 35.3 ± 53.2 (SD) mg C m^{-2} d^{-1}, which compares well with previous estimates in the region measured using sediment traps (60.3 mg C m^{-2} d^{-1}; Redalje et al. 1994), calculated from sediment community oxygen consumption (25.3 mg C m^{-2} d^{-1}; Rowe et al. 2008), and modelled from surface productivity (17.9 mg C m^{-2} d^{-1}; Biggs et al. 2008). The aragonite saturation state and export productivity layers were resampled to match the resolution and extent of the bathymetry data with no additional interpolation.

Fine-scale models

High-resolution bathymetric data were acquired for 7 sites (Fig. 1) in 2008 using a Kongsberg-Simrad EM1002 multibeam echosounder (95 kHz, 111

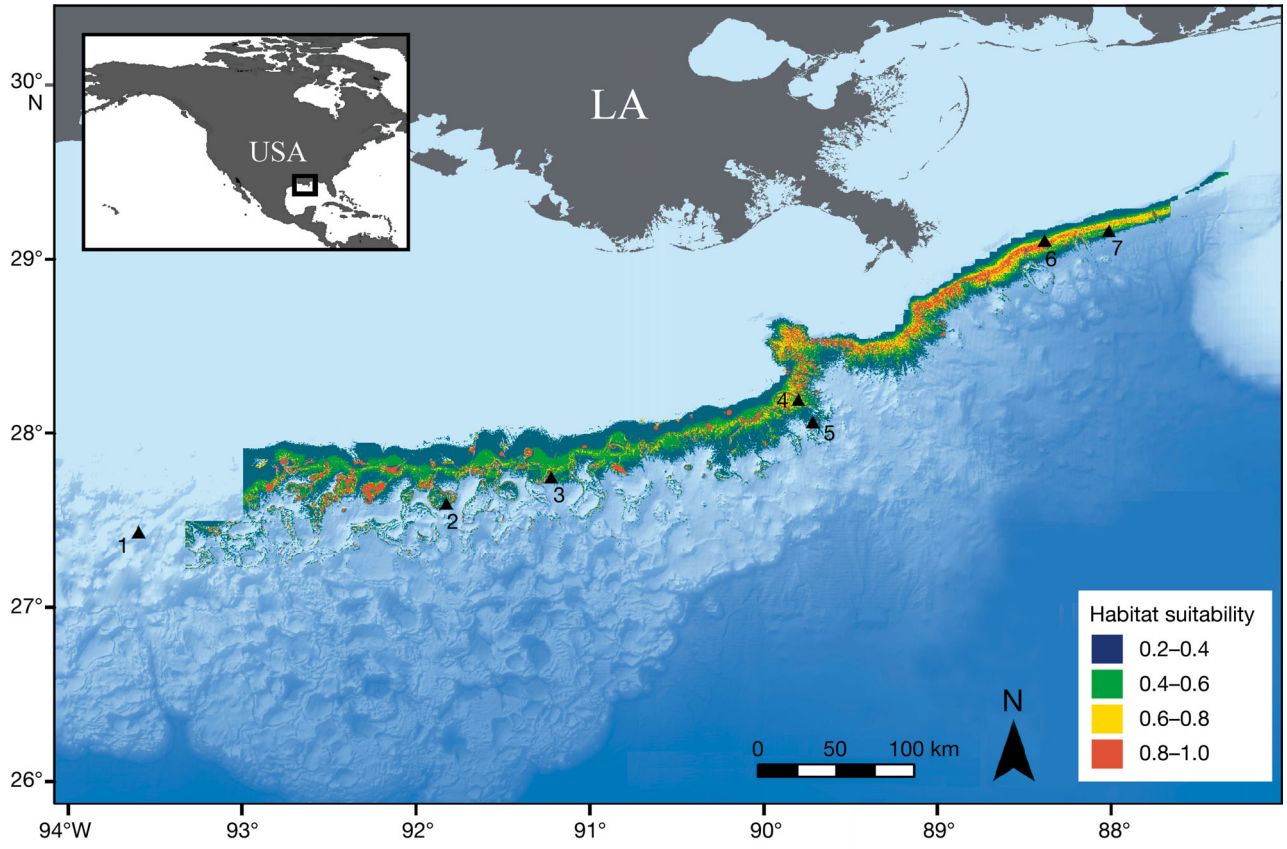

Fig. 1. Broad-scale habitat suitability model for *Lophelia pertusa* in the Gulf of Mexico. Warmer colors (orange to yellow) indicate locations that are predicted to be more suitable (suitability is not shown when less than 0.2). Black triangles indicate the locations of fine-scale sites (west to east: 1–Garden Banks GB535, 2–Green Canyon GC354, 3–Green Canyon GC234, 4–Mississippi Canyon MC751, 5–Mississippi Canyon MC885, 6–Viosca Knoll VK862/VK906, 7–Viosca Knoll VK826)

beams, 150° coverage) mounted on the R/V 'Nancy Foster'. Despite postprocessing, these data contained visible 'ribbing' artifacts that most multibeam data are subject to (Hughes Clarke 2003); however, these imperfections comprised a negligible portion of the data at each site. These data were gridded at their native resolutions of either 5 or 8 m and used to derive the terrain variables slope, aspect, roughness, curvature, and TPI as described above. Surface reflectivity data were available at a high resolution (generally finer than 10 m) from the BOEM database, collected using backscatter from multibeam and side-scan sonar surveys. Each image was georeferenced and then reclassified using a histogram-equalized scheme to categorize surface reflectivity values into 4 classes (very high, high, low, and very low), with higher reflectivity indicating a stronger acoustic return and the presence of more hard substrata. The resulting layers were resampled to match the resolution and extent of the bathymetry with no interpolation.

Model generation

Most traditional methods for modelling species' distributions require both presence and absence data. When high-quality absence data are available, presence-absence models perform slightly better than presence-only models. However, when absence data are of poor quality or potentially unreliable, presence-only models have been proven to be more robust, especially if the species' distribution is not in equilibrium (Hirzel et al. 2001). Obtaining high-quality absence data in the deep sea is usually impossible because of the prohibitive amount of time and expense required for exhaustive exploration and survey. Accordingly, datasets on the absence of deep-sea species are typically sparse and biased because of the limited field of view of the ROV and lack of systematic observations across all of the potentially occupied substrata. Regardless of the environment, habitat suitability predictions from absence data may be inaccurate or misleading

because of dispersal limitation, biotic interactions, detection error, or historical reasons (see Hirzel et al. 2002). Deep-sea ecosystems may be especially prone to the historical removal of organisms from otherwise suitable locations because of anthropogenic disturbances (Fosså et al. 2002, Larsson & Purser 2011). In addition, recent studies have found that presence-only modelling results were in agreement with more traditional presence-absence approaches for both shallow- (Couce et al. 2012) and deep-water corals (Tracey et al. 2011). Therefore, we chose the machine-learning Maxent algorithm (v3.3.3k; Phillips et al. 2006) because it utilizes pseudoabsence (background) data rather than true absence data and has consistently outperformed other traditional (Reiss et al. 2011) and presence-only techniques (Elith et al. 2006, Tittensor et al. 2009, Tong et al. 2013). This approach has been successfully applied in many recent studies modelling the niche of shallow-water (Couce et al. 2012), mesophotic (Bridge et al. 2012), and deep-sea corals (Tittensor et al. 2009, Davies & Guinotte 2011, Quattrini et al. 2013, Rengstorf et al. 2013).

Models were created using default Maxent parameters that have been shown to optimize model performance (convergent threshold = 10^{-5}, number of background points = 10000, default prevalence = 0.5; see Phillips & Dudik 2008) However, the number of maximum iterations was increased to 5000 to ensure convergence, and the regularization multiplier was optimized empirically (see 'Model tuning'). A jackknifing procedure was employed to calculate the percent contribution of variables to each model. Since the data were normally distributed (Shapiro-Wilk, $p = 0.208$), we used a 1-way ANOVA with a Holm-Sidak post hoc test to assess whether predictions differed significantly among surface reflectivity classes for the fine-scale models (SigmaPlot 12.3). The environmental layers used in the broad-scale model all differed significantly from a normal distribution because of their large sample size, even when log transformed (Shapiro-Wilk, $p < 0.01$, $N = 673\,646$). Therefore, the Spearman's rank correlation was calculated between each layer (SigmaPlot 12.3; Table S1 in the Supplement, available at www.int-res.com/articles/suppl/m506p145_supp.pdf). Spearman's correlations were also calculated to determine the relationship between additional metrics that were not normally distributed (Shapiro-Wilk, $p < 0.05$): model performance (area under the curve), sample size, niche breadth, and site area. Since Maxent has been shown to be robust regarding correlated inputs (Phillips et al. 2006, Elith et al. 2011), even highly correlated variables were not removed prior to analysis to avoid biasing the results based on preconceived perceptions of variable importance (see Drake et al. 2006). However, correlated variables should be treated with caution when interpreting the importance of variables in models (Tittensor et al. 2009, Huang et al. 2011). Models produced a continuous raw output for statistical analysis, to which we applied a logistic function to produce a habitat suitability index, which approximates the probability of occurrence at each locality.

Model verification

We employed a cross-validation procedure to verify model performance by randomly partitioning occurrences into 10 calibration and evaluation datasets, using 70% of occurrences for calibration and 30% for evaluation. The predictive ability of all models was assessed with a 1-tailed exact binomial test to determine whether models predict test points better than a random model, using the minimum training threshold to distinguish suitable habitat from nonsuitable habitat (Phillips et al. 2006). The ability of models to accurately predict test data was also assessed using a threshold-independent receiver operating characteristic (ROC) curve, which tests the ability of the model to correctly rank both presences and pseudoabsences (Swets 1988). ROC curves are evaluated by the area under the curve (AUC) metric, which in presence-only models indicates the probability that the model will correctly rank occurrences over background locations. The maximum theoretical AUC in a presence-only model is generally unknowable but always less than 1 if the evaluation data are not independent from the training data, and a random model has a theoretical AUC of 0.5 (Wiley et al. 2003, Phillips et al. 2006).

Sampling bias

To test for sampling bias that may have resulted from targeted exploration during ROV and HOV dives, we used an independently collected dataset of occurrences observed during photographic transects conducted by the autonomous underwater vehicle (AUV) 'Sentry' (Woods Hole Oceanographic Institution) in 2009. Six transects averaging 885 ± 123 (SD) m in length were conducted in the area covering the

large knoll at the center of the VK826 site in an ordered, predetermined fashion. An additional *Lophelia pertusa* model was constructed at VK826 using this dataset (N = 505) and compared to the original model using a Spearman's correlation (SigmaPlot 12.3) and the niche overlap test (ENMTools v1.3; Warren et al. 2008, 2010). The niche overlap test calculates a modified Hellinger distance (van der Vaart 1998), referred to as the *I* metric, that ranges from 0 to 1, with values 0.0–0.2 = 'no or limited' niche overlap, 0.2–0.4 = 'low' overlap, 0.4–0.6 = 'moderate' overlap, 0.6–0.8 = 'high' overlap, and 0.8–1.0 = 'very high' overlap (Rödder & Engler 2011).

Model validation

To test the ability of models to predict occurrences in a new region, each of the fine-scale models generated for other sites was projected onto the VK826 site and evaluated against the independent 'Sentry' dataset of occurrences. The performance of each projected model was evaluated using ROC curves and AUC as above. As a final validation, we ground-truthed specific model predictions at an unexplored region of the VK826 site during an ECOGIG consortium cruise in 2013. Ground-truthing results were analyzed by comparing the original VK826 model to the models projected onto VK826 using only the occurrences obtained from the new region of the site.

Model tuning

Rather than simply using the default settings in Maxent, we optimized the regularization multiplier (β) using a model selection procedure following Warren & Seifert (2011). Regularization is a smoothing function that controls model complexity, with higher values resulting in simpler models with fewer parameters. For each site, we calculated a series of models with regularization multipliers of 1, 3, 5, 7, 9, 11, 13, 15, 17, and 19. The performance of each variant was assessed by calculating a sample size-corrected Akaike Information Criterion (AICc; Warren & Seifert 2011) score, using training data from both the same geographic area and the independent 'Sentry' dataset. The default regularization (β = 1) in Maxent consistently produced the best results when models were verified against training data (Fig. S1a in the Supplement, available at www.int-res.com/articles/suppl/m506p145_supp.pdf). However, when tested against the independent 'Sentry' data at VK826, fine-scale model performance was instead optimized by decreasing model complexity using values for β between 5 and 9 (Fig. S1b in the Supplement). The average performance (AUC) of β-optimized and β-default models was not different when evaluated against test data from the same geographic region (*t*-test, $t = 2.18$, $p = 0.91$), but β-optimized models performed significantly better when tested against the independent 'Sentry' data (Fig. 2, *t*-test, $t = 2.3$, $p < 0.05$). The average performance of default models was lower when evaluated against ground-truthing data, but this decrease was not significant (*t*-test, $t = 2.26$, $p = 0.31$), possibly because of the much smaller sample size (N = 13). To maximize the ability of models to predict occurrences at novel sites, the regularization multiplier that maximized model transferability for each model was used in the generation of all fine-scale models (see Table 1).

Since TPI measures are inherently scale dependent (Rengstorf et al. 2012), we employed a similar model-selection process to determine the scale that optimized model performance. Each model was run using a TPI layer calculated at a scale of 25, 50, 100, 150, 200, 300, 400, 500, 600, 750, and 1000 m, and the relative performance of each model variant was evaluated using AICc scores. For both the broad- and fine-scale models, performance tended to increase when TPI was calculated at broader scales, plateauing after the 500 m scale. In the broad-scale model, TPI calculated at a scale of 750 m exhibited the highest performance by a small margin and was used during subsequent model creation. TPI calculated at a scale of 500 m (TPI-500) optimized model performance in 5 out of 7 fine-scale models: VK826, VK906, GB535, MC751, and GC354 (Fig. S1c in the Supplement). At GC234, TPI did not contribute any information at any scale and therefore had no effect on model performance. Although the 500 m scale was not optimal for GC234, or MC885 where suitability was optimized at a scale of 100 m, we calculated TPI at this scale for all fine-scale models to ensure that the models would be directly comparable.

Niche metrics

We calculated niche breadth in accordance with the inverse concentration metric developed by Levins (1968) using ENMTools (Warren et al. 2008, 2010). Niche breadth essentially describes a species' ability to tolerate deviations from its optimal environmental conditions. Larger values indicate that the

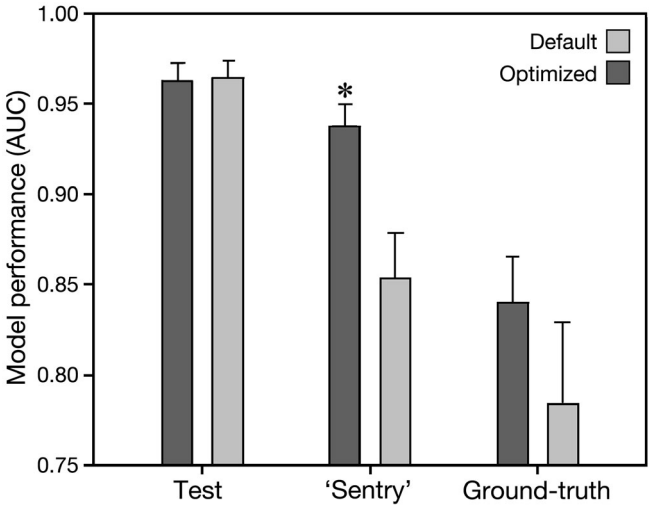

Fig. 2. Average fine-scale model performance (area under the curve, AUC) when model complexity (β) was optimized through a model tuning procedure (dark grey) or left as the default in Maxent (β= 1, light grey), assessed against test occurrences from within each site and against independent autonomous underwater vehicle 'Sentry' and ground-truthing occurrences at the Viosca Knoll VK826 site. Significant differences are marked with an asterisk (*t*-test, 2-tailed, α= 0.05). Error bars indicate standard deviation

species occupies a wider niche space, while smaller values indicate a more specialized niche. The percentage of area predicted to be highly suitable was calculated using a binary prediction of suitability created using the sensitivity–specificity sum maximization approach (Liu et al. 2005), divided by the total area of each site.

Predictive modelling program

To allow researchers who are unfamiliar with modelling techniques to apply our models to their own data to predict *Lophelia pertusa* locations, we incorporated each model into the downloadable program Cold-water Coral Modeler, freely available along with a user's manual on the Cordes website at http://astro.temple.edu/~ecordes/modelling.html. The program was constructed in C# using Microsoft Visual Studio 2012. It utilizes the lambda file created by Maxent during model generation to project a predictive model onto bathymetric data input by the user, generating a habitat suitability map in a novel geographic region.

RESULTS

Broad-scale model

A single model was constructed for *Lophelia pertusa* at a resolution of 25 m for an area of the northern Gulf of Mexico covering approximately 67000 km^2 (Fig. 1). Model performance was excellent, significantly outperforming a random model (exact binomial test, $p < 0.001$) with a high AUC of 0.981 ± 0.001 (Table 1). The presence or absence of hard substrata was the best predictor of *L. pertusa* distribution at the broad scale, contributing 43.0% of information to the model (Table 1). Locations with hard substrata had significantly higher suitability indices than loca-

Table 1. Input data and evaluation for broad- and fine-scale *Lophelia pertusa* models. The regularization multiplier (β) used in each model is listed, along with the number of spatially explicit occurrences used for training, area (km^2) modelled, and niche breadth. Average area under the curve (AUC) ± SD values are shown with significance marked (exact binomial test, *p < 0.01, **p < 0.001). The 2 primary explanatory variables for each model are listed along with the percentage of information contributed by each variable. TPI: topographic position index at a scale of 500 m

Site	Area (km^2)	β	Sample size	Average AUC ± SD	Niche breadth (× 10^{-3})	Suitable area (%)	Variable 1	Variable 2
Viosca Knoll								
VK826	18	5	1242	0.941 ± 0.007**	125.12	4.7	TPI-500 (59.0%)	Depth (39.6%)
VK862/VK906	49	7	425	0.978 ± 0.003**	51.29	1.9	TPI-500 (96.4%)	Roughness (1.6%)
Mississippi Canyon								
MC751	8	5	166	0.983 ± 0.004**	46.11	1.8	Depth (47.7%)	TPI-500 (28.6%)
MC885	63	5	11	0.928 ± 0.025**	233.75	6.3	TPI-500 (49.3%)	Reflectivity (28.1%)
Garden Banks								
GB535	25	7	26	0.992 ± 0.002**	96.53	1.6	TPI-500 (84.1%)	Roughness (11.7%)
Green Canyon								
GC354	10	9	29	0.977 ± 0.019**	189.92	6.3	Reflectivity (40.5%)	Depth (38.5%)
GC234	16	5	15	0.940 ± 0.025*	526.81	3.7	Depth (61.2%)	Reflectivity (38.3%)
Broad scale	67364	1	450	0.981 ± 0.001**	57.08	0.6	Hard bottom (43.0%)	Depth (27.2%)

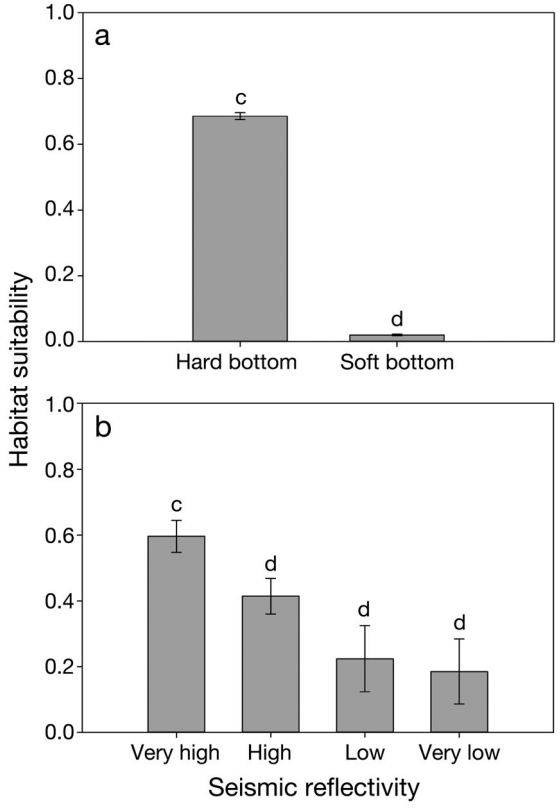

Fig. 3. (a) Average suitability indices for hard and soft bottoms for the broad-scale model. Locations with hard bottoms had significantly higher suitability indices. Different letters above bars indicate significantly different suitability indices (*t*-test, 2-tailed, $\alpha = 0.01$). (b) Response of the predicted habitat suitability to changes in surface reflectivity data, averaged across all fine-scale models. Higher reflectivity indicates the presence of more hard substrata. Different letters above bars indicate significantly different suitability indices (ANOVA $p < 0.01$, post hoc Holm-Sidak $p < 0.05$). Error bars indicate standard deviation

tions with soft substrata (*t*-test, 2-tailed, $p < 0.001$; Fig. 3a). Depth was the secondary explanatory variable in the broad-scale model, contributing 27.2% of information (Table 1). The highest suitability indices for *L. pertusa* occurred between depths of 300 and 600 m (Fig. S2h in the Supplement). Depth was significantly but weakly correlated with TPI calculated at the 750 m scale (Spearman's correlation, $\rho = -0.047$, $p < 0.05$) and the 25 m scale (Spearman's correlation, $\rho = 0.003$, $p < 0.05$; Table S1 in the Supplement). TPI was a good predictor of *L. pertusa* only when calculated at a scale of 750 m (percent contribution of 21.6%). The suitability index was extremely low (<0.05) at negative TPI values but increased rapidly when TPI was positive until reaching a peak at approximately 50, after which it declined (Fig. S3h in the Supplement).

Fine-scale models

Maxent models were constructed for *Lophelia pertusa* at a scale of 5 m at 7 sites in the Gulf of Mexico (VK826, VK862/VK906, MC751, MC885, GB535, GC234, and GC354) (Table 1), visualized as habitat suitability maps (Fig. 4). Verification of models with test data showed that all models were robust. The average test AUC for all sites was 0.963 ± 0.03, with a lowest AUC value of 0.928 ± 0.025 at MC885. All models significantly outperformed a random model (exact binomial test, $p < 0.01$; Table 1). Niche breadth averaged 181.36 ± 167.19 (SD) × 10^{-3} across all sites and ranged from 46.11 × 10^{-3} at MC751 to 526.81 × 10^{-3} at GC234. VK862/VK906, GB535, and GC354 all had intermediate niche breadths of 51.29 × 10^{-3}, 96.53 × 10^{-3}, and 189.92 × 10^{-3}, respectively (Table 1). AUC had a significant negative correlation with niche breadth (Spearman's correlation, $\rho = -0.821$, $p < 0.05$), indicating that models performed better when *L. pertusa* occupied a narrower niche space. The number of occurrences used to train models was strongly but not significantly negatively correlated with niche breadth (Spearman's correlation, $\rho = -0.643$, $p = 0.10$), although this relationship was largely driven by GC234, which had the largest niche breadth (526.81 × 10^{-3}) and the second smallest sample size (N = 15). In general, models trained with more occurrences had higher AUC values, although this relationship was not significant (Spearman's correlation, $\rho = 0.393$, $p = 0.34$), and this pattern did not hold at VK826, which had the largest sample size (N = 1242) and a relatively low AUC of 0.941. Site area (km^2) was not correlated with either niche breadth (Spearman's correlation, $\rho = 0.179$, $p = 0.66$) or AUC (Spearman's correlation, $\rho = -0.286$, $p = 0.49$). At all sites, the area predicted to be highly suitable was extremely low, ranging from 1.6 to 6.3% (Table 1).

In 6 out of 7 fine-scale models, suitability indices for *L. pertusa* were higher at positive TPI values, indicating that elevated seafloor features generally provided better habitat than depressions or flat areas (Fig. S3 in the Supplement). However, suitability peaked prior to the highest TPI value found at 3 of the sites: VK906, MC751, and MC885 (Fig. S3b–d in the Supplement). At GC234, TPI provided no information to the model, and therefore suitability at this site did not vary with TPI values (Fig. S3g in the Supplement). TPI calculated at the 500 m scale was the primary or secondary explanatory variable in 5 out of 7 models, contributing an average of 63.5% of information in those models (Table 1). Roughness was one of the top 2 explanatory variables only at GB535 (percent contribution of

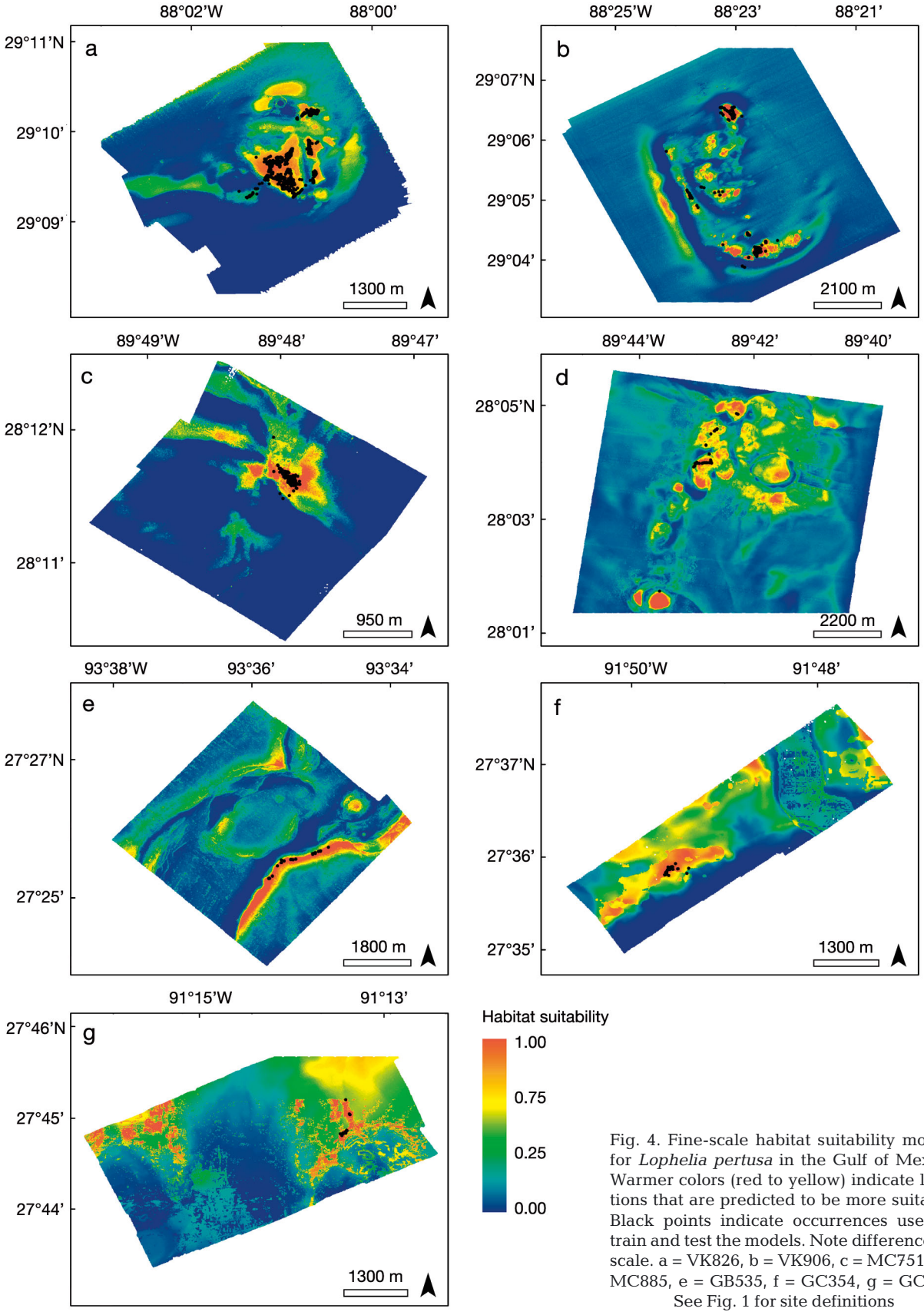

Fig. 4. Fine-scale habitat suitability models for *Lophelia pertusa* in the Gulf of Mexico. Warmer colors (red to yellow) indicate locations that are predicted to be more suitable. Black points indicate occurrences used to train and test the models. Note differences in scale. a = VK826, b = VK906, c = MC751, d = MC885, e = GB535, f = GC354, g = GC234. See Fig. 1 for site definitions

11.7%) and VK906 (percent contribution of 1.6%) and had negligible contributions to other fine-scale models. At all sites, suitability increased with roughness but generally plateaued around values of 1.2 (data not shown), which indicates a relatively flat surface.

Depth was the primary or secondary explanatory variable in 4 out of 7 *L. pertusa* models, contributing an average of 46.8% of information in those models (Table 1). Suitability indices tended to be higher in the shallower regions of each site, with the highest index values between depths of approximately 300 and 600 m, matching the most common depth range for *L. pertusa* in the Gulf of Mexico (Fig. S2a–g in the Supplement). Surface reflectivity was the primary explanatory variable at GC354, contributing 40.5% of information, and was the secondary explanatory variable at MC885 and GC234, contributing 28.1% and 38.3% of information, respectively. Locations with very high reflectivity values had significantly higher suitability indices than sites with high, low, or very low reflectivity values (ANOVA $p < 0.01$, post hoc Holm-Sidak $p < 0.05$; Fig. 3b).

Test for sampling bias

An additional *Lophelia pertusa* model was constructed at VK826 using independent data obtained from AUV 'Sentry' transects as a general test for sampling bias. This model had a test AUC of 0.958 ± 0.004 and significantly outperformed a random model (exact binomial test, $p < 0.01$). The test model was significantly correlated with the original VK826 model (Spearman's correlation, $\rho = 0.938$, $p < 0.01$), and the models had a 'very high' level of niche overlap ($I = 0.97$).

Model validation

All fine-scale models projected onto the VK826 site (Fig. S4 in the Supplement) performed reasonably well when tested against the independent 'Sentry' dataset, with AUC values ranging from 0.878 to 0.972 and an average AUC of 0.937 ± 0.033 (Fig. 2, Table 2). Not surprisingly, the original VK826 model had the highest AUC (0.972) when tested against the independent 'Sentry' data and had the highest correlation (Spearman's correlation, $\rho = 0.938$, $p < 0.01$) and overlap ($I = 0.97$) with the 'Sentry' model. The MC751 model had 'moderate' niche overlap ($I = 0.46$) and had the weakest correlation with the 'Sentry' model, although significance was obtained because of the extremely large sample size (Spearman's correlation, $\rho = 0.256$, $p < 0.01$, $N = 729230$). The remaining models were all significantly and moderately to highly correlated with the 'Sentry' model and exhibited 'high' or 'very high' niche overlap (Table 2). Visually, the projected models generally matched well with both the original VK826 model and with the known distribution of *Lophelia pertusa* at the site but had a tendency to overpredict suitability (Fig. S4 in the Supplement).

Table 2. Evaluation of fine-scale models projected onto the VK826 site and validated against both the independent autonomous underwater vehicle 'Sentry' data and ground-truthing data. The area under the curve (AUC) of each model is shown, along with the Spearman's correlation (ρ, $p < 0.01$) and niche overlap (I) with the original VK826 model

Site	AUC		Spearman's ρ	Overlap (I)
	'Sentry'	Ground truth		
Viosca Knoll				
VK826	0.972	0.928	0.938	0.970
VK862/VK906	0.961	0.881	0.813	0.891
Mississippi Canyon				
MC751	0.926	0.769	0.256	0.456
MC885	0.952	0.847	0.564	0.714
Garden Banks				
GB535	0.958	0.891	0.643	0.895
Green Canyon				
GC354	0.914	0.820	0.550	0.782
GC234	0.878	0.742	0.643	0.721

The VK826 model predicted several areas of high suitability that had not been previously surveyed at this site. Ground-truthing of specific model predictions at the VK826 site resulted in the discovery of 2 large *L. pertusa* mounds. The VK826 model had an AUC of 0.928 when tested using *L. pertusa* location data from the ground-truthing area of the site ($N = 13$). Models projected onto VK826 exhibited much poorer performance when tested against ground-truthing data (Fig. 2) but still outperformed a random model (exact binomial test, $p < 0.01$) and had a reasonable ability to discriminate with an average AUC of 0.840 ± 0.067 (Table 2). AUC scores calculated from 'Sentry' data were highly correlated with scores calculated using ground-truthing data (Spearman's correlation, $\rho = 0.929$, $p < 0.01$).

DISCUSSION

Ecological niche models were developed at 2 scales to assess the niche of *Lophelia pertusa* in the northern Gulf of Mexico and to facilitate discovery of

L. pertusa at sites that have only been explored using remotely sensed data. Fine-scale models built at a high resolution (5 m) using only topographic variables and surface reflectivity data were sufficient to accurately quantify *L. pertusa*'s niche within sites and predict occurrences in a different geographic area. Collecting ship-based multibeam bathymetry and surface reflectivity data is relatively inexpensive and rapid compared to surveying regions using ROVs or HOVs; when coupled with the ecological niche models developed here, this approach is capable of greatly increasing the efficiency of future expeditions. On average, a very small fraction of the modelled area (less than 7% for all models) was predicted to be highly suitable, greatly narrowing down potential dive targets in new regions.

The higher suitability indices observed at positive TPI values demonstrated that *L. pertusa* has a clear preference for more complex, elevated topography and indicated that depressions and flat areas generally comprise substandard habitat. Elevated regions increase local current speeds, boosting the transport of food and nutrients (Thiem et al. 2006), increasing larval supply (Piepenburg & Müller 2004), and reducing sediment deposition (Rogers 1994). These results were not surprising, as previous work has often associated the presence of *L. pertusa* and other cold-water corals with steep, elevated, and complex topography even at broader scales (e.g. Bryan & Metaxas 2006, Davies et al. 2008, but see Tittensor et al. 2009), an association known as the 'enhanced current hypothesis' (see Masson et al. 2003). However, suitability indices reached their largest values before the largest TPI value observed at 3 of the sites (Fig. S3 in the Supplement), indicating that there may be an obstacle to colonization or survival at the topographic peaks of some sites. These findings are consistent with recent studies that recorded reduced diversity on the summits of seamounts relative to the surrounding slopes, thought to be influenced in part by extreme hydrological forces, exposure to oxygen-minimum zones, or the fine-scale topography of the summit (see review by Clark et al. 2010). At sites with large mound structures, such as the salt domes of the Gulf of Mexico, the summits may experience dramatically accelerated currents that have been shown to prevent the recruitment of other invertebrate larvae (e.g. Mullineaux & Garland 1993) and negatively affect *L. pertusa* feeding rates (Purser et al. 2010). Alternatively, it is plausible that since locations with extremely high TPI values were not as common at most sites, they were less likely to be inhabited simply by chance.

In both fine- and broad-scale models, *L. pertusa* was generally predicted to be prevalent only where there were hard substrata. This finding confirms previous work suggesting that *L. pertusa* and other coral species require hard substrata for the initial attachment and recruitment of larvae (Wilson 1979, Gass & Roberts 2006) and may largely explain the absence of corals at locations that are otherwise suitable. The lack of hard substrata has been previously suggested to limit the size and density of *L. pertusa* reefs in the northeastern Atlantic (Long et al. 1999) and may be similarly limiting populations in the Gulf of Mexico given the reduced suitability at locations with soft bottoms.

Depth was commonly the most important variable in models. However, it seems likely that the importance of depth was caused by covarying factors such as carbonate chemistry and export productivity, which both contributed surprisingly little information to the broad-scale model. The aragonite saturation state has been shown to be extremely influential on the growth and survival of cold-water corals in experimental (Maier et al. 2009), field (Lunden et al. 2013), and modelling studies (Tittensor et al. 2009, Quattrini et al. 2013). It is important to note, however, that *L. pertusa* only occurred in a narrow range of saturation states (1.25 to 1.69) in this study. Previous work that found a preference for higher saturation states documented occurrences across a much broader range of values (e.g. Davies & Guinotte 2011).

Export productivity was similarly unimportant in the broad-scale model, despite the clear importance of food supply to coral growth and survival. As with aragonite saturation state, this may be partially because of its intrinsic relationship with depth or may be the result of a spatial offset between surface productivity and benthic food supply. In the northern Gulf of Mexico, the lateral transport of POC by advection contributes significantly to the available POC pool at the seafloor, particularly near the outflow of the Mississippi River (Rowe et al. 2008). Given the similar lack of importance of export productivity in other modelling studies (Tittensor et al. 2009, Davies & Guinotte 2011), it may be beneficial to incorporate direct measurements of POC flux and resuspension rates at depth to more accurately capture fine-scale variability in food availability.

Many other environmental factors that partially correlate with depth, including temperature, salinity, and dissolved oxygen, did not exist at a high enough spatial resolution or on a long enough time series to be included here but are also likely to be important components of *L. pertusa*'s niche. These factors may

also affect *L. pertusa*'s modelled niche breadth (e.g. Davies et al. 2008), which varied considerably among sites in this study. More work is needed to more accurately determine *L. pertusa*'s niche breadth in the Gulf of Mexico and elsewhere, as this metric has substantial ecological implications. Niche breadth represents a potential tradeoff between habitat use and growth; generalist species gain the ability to occupy more habitats but frequently have reduced growth rates (Caley & Munday 2003). In addition, more specialized species with a smaller niche breadth have been shown to be more sensitive to the loss in suitable habitat caused by climate change (Thuiller et al. 2005). As these environmental data continue to be mapped with higher precision in the deep Gulf of Mexico, it may be possible to delineate how these variables affect *L. pertusa*'s distribution and niche breadth and to model the potential loss in suitable habitat under future scenarios involving ocean acidification, warming, or deoxygenation.

Both fine- and broad-scale models reflected the known biogeography and ecology of *L. pertusa* but refined our understanding of the scale at which these variables operate. Despite the broad-scale topography often included in modelling studies (e.g. Tittensor et al. 2009, Davies & Guinotte 2011, Ross & Howell 2013), there is evidence to suggest that fine-scale features may be more important for successful recruitment and growth. For example, Roberts et al. (2003) found that mounds less than 10 m in diameter frequently corresponded with large *L. pertusa* colonies, and a study in Irish waters found that a 1000 m grid size was insufficient to adequately detect carbonate mounds in the region (Rengstorf et al. 2012). Similarly, a scale of 750 m failed to predict known *L. pertusa* occurrences on fine-scale features (Ross & Howell 2013). The high-resolution bathymetry used here further reveals the potential of relatively small features to affect coral distribution, likely through modification of local current regimes. Only Dolan et al. (2008) used higher resolution terrain data (grid size of 0.5 m) in their modelling study of cold-water corals on the Irish continental slope. However, their study required an ROV-mounted sonar system and therefore could not predict occurrences in new regions unless such high-resolution data were already available or obtained using near-bottom surveys.

Terrain attributes are inherently scale dependent. Choosing the appropriate scale of analysis ultimately depends on the environmental heterogeneity that organisms respond to, which is likely to be highly dependent on the study area and the variable in question (Wiens 1989). In this study, TPI calculated at a broad scale (500 or 750 m) tended to optimize model performance in both the broad- and fine-scale models. Rather than reflecting an inherent niche requirement of *L. pertusa*, these likely were simply the most appropriate scales to characterize the large carbonate mounds found at many sites, which are generally wider than 500 m. In regions with smaller or larger mounds, a different scale may be more appropriate. For example, the MC885 site contains a series of smaller mounds (<200 m in diameter), and TPI was optimized at the 100 m scale at this site. Given these results, it appears to be important to ensure that the analysis scale is within the same scale domain of the target features within the study area. Rengstorf et al. (2012) conducted a multiscale terrain analysis to model *L. pertusa*'s niche in the northeastern Atlantic but only included resolutions from 50 to 1000 m in their analysis and did not quantify the effect of scale on model performance. A more detailed multiscale study (e.g. Wilson et al. 2007) that quantifies how a broad range of scales affects model performance is the next step toward more fully characterizing *L. pertusa*'s niche in the Gulf of Mexico and elsewhere.

While many ecological niche studies have relied solely on model verification, recent work highlights the importance of employing true model validation when possible by testing models with independent data in a neighboring geographic region (Araújo & Guisan 2006). The performance of models in this study was considerably reduced when they were projected to a new region and tested using an independent dataset; however, the projected models still performed reasonably well and can therefore be expected to be of value at truly unexplored sites. It is important to note, however, that we validated our models within the same geographic region, and our results will not necessarily extrapolate as well to other portions of the Gulf of Mexico or other ocean basins. More work is needed to determine if *L. pertusa* occupies a similar niche space in different biogeographic regions. This validation schema also provided a useful framework to test how modifying the regularization multiplier affected model performance. We found that the default settings generated relatively complex models that were heavily biased toward performing well under model verification but had reduced performance when validated against independent data in a neighboring geographic region. In addition to increasing the transferability of models to new regions or time periods, increasing the regularization multiplier results in more parsimonious models that are less likely to overfit training

data and are easier to interpret biologically (see Warren & Seifert 2011). The verification of the prediction of 2 previously unknown *L. pertusa* mounds within the relatively well explored VK826 site further validates the accuracy of this approach and highlights the potential utility of fine-scale models.

Despite the high performance of all models, there were relatively large regions that were predicted to be suitable but are not currently known to be inhabited. It is possible that the models simply overestimated the suitable habitat for each species. Niche models rely on the theory that a species' distribution is largely driven by the portions of its ecological niche that can be readily quantified. While there is ample evidence for this theory (see Schoener 1989), it is also clear that other factors, such as disease, seasonal variability, climate change, or resource availability, may partially structure distributions and reduce the size of the realized niche. Unfortunately, most of these factors are currently intractable in modelling efforts, especially in the deep sea. In addition, many assumptions of niche theory are often violated out of necessity during model construction. If species' distributions are not in equilibrium, dispersal is limiting, the niche is diverging, or biotic interactions strongly influence distribution, then niche models will be inherently inaccurate (see review by Wiens et al. 2009). Given these considerations, it is plausible that unoccupied regions that were predicted to be suitable may be unsuitable in reality because of any number of factors that could not be included during model creation and that further field surveys and modelling efforts may greatly increase our understanding of *L. pertusa*'s distribution. However, many unfilled locations occurred in regions that have not been well surveyed, and it seems likely that extensive cold-water coral populations remain to be discovered in the Gulf of Mexico.

CONCLUSION

The lack of information concerning the distribution of cold-water corals in the Gulf of Mexico represents a serious obstacle to research and conservation efforts in the region. In this study, we used ecological niche models to quantify the niche of the cold-water *Lophelia pertusa* and to predict its occurrence throughout the northern Gulf of Mexico. Modelling results revealed that *L. pertusa*'s distribution was primarily driven by depth, locally elevated topography, and the need for hard substrata suitable for recruitment. These results were not surprising given our existing knowledge of cold-water coral distribution and habitat preference, but our multiscale, high-resolution niche modelling approach allowed us to precisely quantify *L. pertusa*'s niche and provide a more inexpensive and accurate method for locating novel coral sites. The habitat suitability maps presented here will also inform management efforts, a particular concern in the Gulf of Mexico because of heavy oil and natural gas exploration and extraction activities and threats from other forms of anthropogenic disturbance including ocean acidification and deep-water fishing. Therefore, we suggest that future expeditions and resource management planning in the deep Gulf of Mexico and elsewhere combine remotely sensed data with these models to better understand what constitutes suitable habitat for *L. pertusa* and other cold-water corals and to predict their distribution in unexplored regions.

Acknowledgements. Funding was provided by BOEM and NOAA OER (BOEM Contract No. M08PC20038) awarded to TDI-Brooks International for the *Lophelia* II project and by the Gulf of Mexico Research Institute to the ECOGIG consortium (ECOGIG Contribution No. 273). This work would not have been possible without support from ship crews of the R/V 'Ronald H. Brown', 'Seward Johnson', and 'Nancy Foster' and the exploration vessel 'Nautilus', as well as the 'Jason II' ROV crew, the 'Johnson-Sea-Link' HOV crew, the 'Hercules' ROV crew, and the 'Sentry' AUV crew. H. Fowle and N. Remon helped analyze video datasets, and M. Kurman analyzed the 'Sentry' phototransects. Special thanks to M. Georgian and K. Piciulo for programming the Cold-water Coral Modeller program. The bathymetry and seismic data are publicly available and are deposited along with the model code in the GoMRI database under GRIIDC ID number R1.x132.141:0004. S.E.G. was funded by the National Science Foundation (NSF) Graduate Research Fellowship Program under Grant No. DGE-1144462. Any opinions, findings, and conclusions or recommendations expressed in this material are those of the authors and do not necessarily reflect the views of the NSF.

LITERATURE CITED

Araújo MB, Guisan A (2006) Five (or so) challenges for species distribution modelling. J Biogeogr 33:1677–1688

Behrenfeld MJ, Falkowski PG (1997) Photosynthetic rates derived from satellite-based chlorophyll concentration. Limnol Oceanogr 42:1–20

Biggs DC, Hu C, Müller-Karger FE (2008) Remotely sensed sea-surface chlorophyll and POC flux at Deep Gulf of Mexico Benthos sampling stations. Deep-Sea Res Part II 55:2555–2562

Bridge T, Beaman R, Done T, Webster J (2012) Predicting the location and spatial extent of submerged coral reef habitat in the Great Barrier Reef World Heritage Area, Australia. PLoS ONE 7

Bryan TL, Metaxas A (2006) Distribution of deep-water corals along the North American continental margins:

relationships with environmental factors. Deep-Sea Res Part I 53:1865–1879

Bryant WR, Bryant JR, Feeley MH, Simmons GR (1990) Physiographic and bathymetric characteristics of the continental slope, northwest Gulf of Mexico. Geo-Mar Lett 10:182–199

Buhl-Mortensen L, Vanreusel A, Gooday AJ, Levin LA and others (2010) Biological structure as a source of habitat heterogeneity and biodiversity on the deep ocean margins. Mar Ecol 31:21–50

Caley MJ, Munday PL (2003) Growth trades off with habitat specialization. Proc R Soc Lond B 270:S175–S177

Carr ME, Friedrichs MAM, Schmeltz M, Aita MN and others (2006) A comparison of global estimates of marine primary production from ocean color. Deep-Sea Res Part II 53:741–770

Clark MR, Rowden AA, Schlacher S, Williams A and others (2010) The ecology of seamounts: structure, function, and human impacts. Annu Rev Mar Sci 2:253–278

Cordes EE, McGinley MP, Podowski EL, Becker EL, Lessard-Pilon S, Viada ST, Fisher CR (2008) Coral communities of the deep Gulf of Mexico. Deep-Sea Res Part I 55:777–787

Costello MJ, McCrea M, Freiwald A, Lundälv T and others (2005) Role of cold-water *Lophelia pertusa* coral reefs as fish habitat in the NE Atlantic. In: Freiwald A, Roberts JM (eds) Cold-water corals and ecosystems. Springer-Verlag, Berlin, p 77–805

Couce E, Ridgwell A, Hendy EJ (2012) Environmental controls on the global distribution of shallow-water coral reefs. J Biogeogr 39:1508–1523

Davies AJ, Guinotte JM (2011) Global habitat suitability for framework-forming cold-water corals. PLoS ONE 6: e18483

Davies AJ, Wisshak M, Orr JC, Roberts JM (2008) Predicting suitable habitat for the cold-water coral *Lophelia pertusa* (Scleractinia). Deep-Sea Res Part I 55:1048–1062

Davies AJ, Duineveld GCA, van Weering TCE, Mienis F and others (2010) Short-term environmental variability in cold-water coral habitat at Viosca Knoll, Gulf of Mexico. Deep-Sea Res Part I 57:199–212

De Mol B, Van Rensbergen P, Pillen S, Van Herreweghe H and others (2002) Large deep-water coral banks in the Porcupine Basin, southwest of Ireland. Mar Geol 188: 193–231

Deuser WG (1986) Seasonal and interannual variations in deep-water particle fluxes in the Sargasso Sea and their relation to surface hydrography. Deep-Sea Res Part I 33: 225–246

Dolan MFJ, Grehan AJ, Guinan JC, Brown C (2008) Modelling the local distribution of cold-water corals in relation to bathymetric variables: adding spatial context to deep-sea video data. Deep-Sea Res Part I 55:1564–1579

Dorschel B, Hebbeln D, Foubert A, White M, Wheeler AJ (2007) Hydrodynamics and cold-water coral facies distribution related to recent sedimentary processes at Galway Mound west of Ireland. Mar Geol 244:184–195

Drake JM, Randin C, Guisan A (2006) Modelling ecological niches with support vector machines. J Appl Ecol 43: 424–432

Elith J, Graham CH, Anderson RP, Dudík M and others (2006) Novel methods improve prediction of species' distributions from occurrence data. Ecography 29:129–151

Elith J, Phillips SJ, Hastie T, Dudík M, Chee YE, Yates CJ (2011) A statistical explanation of MaxEnt for ecologists. Divers Distrib 17:43–57

Eppley RW (1972) Temperature and phytoplankton growth in the sea. Fish Bull 70:1063–1085

Evans IS (1980) An integrated system of terrain analysis and slope mapping. Z Geomorphol 36:274–295

Fleming MD, Hoffer RM (1979) Machine processing of Landsat MSS data and DMA topographic data for forest cover type mapping. LARS Tech Rep 062879. Laboratory for Applications of Remote Sensing, Purdue University, West Lafayette, IN

Fosså JH, Mortensen PB, Furevik DM (2002) The deep-water coral *Lophelia pertusa* in Norwegian waters: distribution and fishery impacts. Hydrobiologia 471:1–12

Freiwald A, Wilson JB, Henrich R (1999) Grounding Pleistocene icebergs shape recent deep-water coral reefs. Sediment Geol 125:1–8

Gage JD (2004) Diversity in deep-sea benthic macrofauna: the importance of local ecology, the larger scale, history and the Antarctic. Deep-Sea Res Part II 51:1689–1708

Gass SE, Roberts JM (2006) The occurrence of the cold-water coral *Lophelia pertusa* (Scleractinia) on oil and gas platforms in the North Sea: colony growth, recruitment and environmental controls on distribution. Mar Pollut Bull 52:549–559

Gjerde KM (2006) Ecosystems and biodiversity report in deep waters and high seas. UNEP Reg Seas Rep Stud No. 178. UNEP/ICUN, Gland

Glover AG, Smith CR (2003) The deep-sea floor ecosystem: current status and prospects of anthropogenic change by the year 2025. Environ Conserv 30:219–241

Guinan J, Brown C, Dolan MFJ, Grehan AJ (2009) Ecological niche modelling of the distribution of cold-water coral habitat using underwater remote sensing data. Ecol Inform 4:83–92

Guinotte JM, Fabry VJ (2008) Ocean acidification and its potential effects on marine ecosystems. Ann N Y Acad Sci 1134:320–342

Guinotte JM, Orr J, Cairns S (2006) Will human-induced changes in seawater chemistry alter the distribution of deep-sea scleractinian corals? Front Ecol Environ 4: 141–146

Hirzel AH, Helfer V, Metral F (2001) Assessing habitat suitability models with a virtual species. Ecol Modell 145: 111–121

Hirzel AH, Hausser J, Chessel D, Perrin N (2002) Ecological-niche factor analysis: How to compute habitat-suitability maps without absence data? Ecology 83:2027–2036

Horn BKP (1981) Hill shading and the reflectance map. Proc IEEE 69:14–47

Howell KL, Holt R, Endrino IP, Stewart H (2011) When the species is also a habitat: comparing the predictively modelled distributions of *Lophelia pertusa* and the reef habitat it forms. Biol Conserv 144:2656–2665

Huang Z, Brooke B, Li J (2011) Performance of predictive models in marine benthic environments based on predictions of sponge distribution on the Australian continental shelf. Ecol Inform 6:205–216

Hughes Clarke JE (2003) Dynamic motion residuals in swath sonar data: ironing out the creases. Int Hydrogr Rev 4: 6–23

Jenness JS (2004) Calculating landscape surface area from digital elevation models. Wildl Soc Bull 32:829–839

Jenness JS (2013) DEM Surface Tools. Jenness Enterprises. Available at: www.jennessent.com/arcgis/surface_area.htm

Jenness JS, Brost B, Beier P (2013) Land Facet Corridor Designer. Jenness Enterprises. Available at: www.jennessent.com/arcgis/land_facets.htm

Jones KH (1998) A comparison of algorithms used to compute hill slope as a property of the DEM. Comput Geosci 24:315–323

Kostylev VE, Erlandsson J, Ming MY, Williams GA (2005) The relative importance of habitat complexity and surface area in assessing biodiversity fractal application on rocky shores. Ecol Complex 2:272–286

Larcom EA, McKean D, Brooks JM, Fisher CR (2013) Growth rates, densities, and distribution of *Lophelia pertusa* on artificial structures in the Gulf of Mexico. Deep-Sea Res Part I 85:101–109

Larsson AI, Purser A (2011) Sedimentation on the cold-water coral *Lophelia pertusa*: cleaning efficiency from natural sediments and drill cuttings. Mar Pollut Bull 62: 1159–1168

Levins R (1968) Evolution in changing environments: some theoretical explorations. Princeton University Press, Princeton, NJ

Liu CR, Berry PM, Dawson TP, Pearson RG (2005) Selecting thresholds of occurrence in the prediction of species distributions. Ecography 28:385–393

Long D, Roberts JM, Gillespie EJ (1999) Occurrences of *Lophelia pertusa* on the Atlantic margin. Br Geol Surv Tech Rep WB/99/24, Edinburgh

Lunden JJ, Georgian SE, Cordes EE (2013) Aragonite saturation states at cold-water coral reefs structured by *Lophelia pertusa* in the northern Gulf of Mexico. Limnol Oceanogr 58:354–362

Maier C, Hegeman J, Weinbauer MG, Gattuso JP (2009) Calcification of the cold-water coral *Lophelia pertusa* under ambient and reduced pH. Biogeosciences 6: 1671–1680

Masson DG, Bett BJ, Billett DSM, Jacobs CL, Wheeler AJ, Wynn RB (2003) The origin of deep-water, coral-topped mounds in the northern Rockall Trough, northeast Atlantic. Mar Geol 194:159–180

Mienis F, Duineveld GCA, Davies AJ, Ross SW, Seim H, Bane J, van Weering TCE (2012) The influence of near-bed hydrodynamic conditions on cold-water corals in the Viosca Knoll area, Gulf of Mexico. Deep-Sea Res Part I 60:32–45

Mohn C, Beckmann A (2002) Numerical studies on flow amplification at an isolated shelfbreak bank, with application to Porcupine Bank. Cont Shelf Res 22: 1325–1338

Montagna PA, Baguley JG, Cooksey C, Hartwell I and others (2013) Deep-sea footprint of the Deepwater Horizon blowout. PLoS ONE 8:e70540

Moore ID, Grayson RB, Ladson AR (1991) Digital terrain modelling: a review of hydrological, geomorphological, and biological applications. Hydrol Process 5:3–30

Morel A, Berthon JF (1989) Surface pigments, algal biomass profiles, and potential production of the euphotic layer: relationships reinvestigated in view of remote-sensing applications. Limnol Oceanogr 34:1545–1562

Morrison CL, Ross SW, Nizinski MS, Brooke S and others (2011) Genetic discontinuity among regional populations of *Lophelia pertusa* in the North Atlantic Ocean. Conserv Genet 12:713–729

Mullineaux LS, Garland ED (1993) Larval recruitment in response to manipulated field flows. Mar Biol 116: 667–683

Orejas C, Gori A, Iacono CL, Puig P, Gili JM, Dale MRT (2009) Cold-water corals in the Cap de Creus canyon, northwestern Mediterranean: spatial distribution, density, and anthropogenic impact. Mar Ecol Prog Ser 397:37–51

Pace ML, Knauer GA, Karl DM, Martin JH (1987) Primary production, new production and vertical flux in the eastern Pacific Ocean. Nature 325:803–804

Pearman PB, Guisan A, Broennimann O, Randin CF (2008) Niche dynamics in space and time. Trends Ecol Evol 23: 149–158

Phillips SJ, Dudik M (2008) Modeling of species distributions with Maxent: new extensions and a comprehensive evaluation. Ecography 31:161–175

Phillips SJ, Anderson RP, Schapire RE (2006) Maximum entropy modeling of species geographic distributions. Ecol Modell 190:231–259

Piepenburg D, Müller B (2004) Distribution of epibenthic communities on the Great Meteor seamount (NE Atlantic) mirrors pelagic processes. Arch Fish Mar Res 51:55–70

Porres de la Haza MJ, Pardo Pascual JE (2002) Comparison between the different curvature models of terrain for determining the degree of soil humidity. In: Sobrino JA (ed) Recent advances in quantitative remote sensing. Publicacions de la Universitat de València, Spain, p 238–245

Purser A, Larsson AI, Thomsen L, van Oevelen D (2010) The influence of flow velocity and food concentration on *Lophelia pertusa* (Scleractinia) zooplankton capture rates. J Exp Mar Biol Ecol 395:55–62

Quattrini AM, Georgian SE, Byrnes L, Falco R, Stevens A, Cordes EE (2013) Niche divergence by deep-sea octocorals in the genus *Callogorgia* across the upper continental slope of the Gulf of Mexico. Mol Ecol 22:4123–4140

Redalje DG, Lohrenz SE, Fahnenstiel GL (1994) The relationship between primary production and the vertical export of particulate organic matter in a river-impacted coastal ecosystem. Estuaries 17:829–838

Reiss H, Cunze S, Koenig K, Neumann H, Kroencke I (2011) Species distribution modelling of marine benthos: a North Sea case study. Mar Ecol Prog Ser 442:71–86

Rengstorf AM, Grehan A, Yesson C, Brown C (2012) Towards high-resolution habitat suitability modeling of vulnerable marine ecosystems in the deep-sea: resolving terrain attribute dependencies. Mar Geod 35:343–361

Rengstorf AM, Yesson C, Brown C, Grehan AJ (2013) High-resolution habitat suitability modelling can improve conservation of vulnerable marine ecosystems in the deep sea. J Biogeogr 40:1702–1714

Roberts JM, Long D, Wilson JB, Mortensen PB, Cage JD (2003) The cold-water coral *Lophelia pertusa* (Scleractinia) and enigmatic seabed mounds along the northeast Atlantic margin: Are they related? Mar Pollut Bull 46:7–20

Roberts JM, Wheeler AJ, Freiwald A (2006) Reefs of the deep: the biology and geology of cold-water coral ecosystems. Science 312:543–547

Roberts JM, Wheeler AJ, Freiwald A, Cairns SD (2009) Cold-water corals: the biology and geology of deep-sea coral habitats. Cambridge University Press, Cambridge

Roberts JJ, Best BD, Dunn DC, Treml EA, Halpin PN (2010) Marine Geospatial Ecology Tools: an integrated framework for ecological geoprocessing with ArcGIS, Python, R, MATLAB, and C++. Environ Model Softw 25: 1197–1207

Rödder D, Engler JO (2011) Quantitative metrics of overlaps in Grinnellian niches: advances and possible drawbacks. Glob Ecol Biogeogr 20:915–927

Rogers AD (1994) The biology of seamounts. Adv Mar Biol 30:305–350

Ross RE, Howell KL (2013) Use of predictive habitat modelling to assess the distribution and extent of the current protection of 'listed' deep-sea habitats. Divers Distrib 19: 433–445

Rowe GT, Morse J, Nunnally C, Boland GS (2008) Sediment community oxygen consumption in the deep Gulf of Mexico. Deep-Sea Res Part II 55:2686–2691

Schoener A (1989) The ecological niche. In: Cherret JM (ed) Ecological concepts. Blackwell Science, Oxford, p 79–114

Schröder-Ritzrau A, Freiwald A, Mangini A (2005) U/Th-dating of deep-water corals from the eastern North Atlantic and the western Mediterranean Sea. In: Freiwald A, Roberts JM (eds) Cold-water corals and ecosystems. Springer, Berlin, p 157–172

Schroeder WW (2002) Observations of *Lophelia pertusa* and the surficial geology at a deep-water site in the northeastern Gulf of Mexico. Hydrobiologia 471:29–33

Schroeder WW, Brooke SD, Olson JB, Phaneuf B, McDonough JJ III, Etnoyer P (2005) Occurrence of deep-water *Lophelia pertusa* and *Madrepora oculata* in the Gulf of Mexico. In: Freiwald A, Roberts JM (eds) Cold-water corals and ecosystems. Springer, Berlin, p 297–307

Swets JA (1988) Measuring the accuracy of diagnostic systems. Science 240:1285–1293

Thiem Ø, Ravagnan E, Foss JH, Berntsen J (2006) Food supply mechanisms for cold-water corals along a continental shelf edge. J Mar Syst 60:207–219

Thuiller W, Lavorel S, Araújo MB (2005) Niche properties and geographical extent as predictors of species sensitivity to climate change. Glob Ecol Biogeogr 14:347–357

Tittensor DP, Baco AR, Brewin PE, Clark MR and others (2009) Predicting global habitat suitability for stony corals on seamounts. J Biogeogr 36:1111–1128

Tong R, Purser A, Guinan J, Unnithan V (2013) Modeling the habitat suitability for deep-water gorgonian corals based on terrain variables. Ecol Inform 13:123–132

Tracey DM, Rowden AA, Mackay KA, Compton T (2011) Habitat-forming cold-water corals show affinity for seamounts in the New Zealand region. Mar Ecol Prog Ser 430:1–22

Turley CM, Roberts JM, Guinotte JM (2007) Corals in deep-water: Will the unseen hand of ocean acidification destroy cold-water ecosystems? Coral Reefs 26:445–448

van der Vaart AW (1998) Asymptotic statistics. Cambridge University Press, Cambridge

van Weering TCE, De Haas H, De Stigter HC, Lykke-Anderson H, Kouvaev I (2003) Structure and development of giant carbonate mounds at the SW and SE Rockall Trough margins, NE Atlantic Ocean. Mar Geol 198: 67–81

Wang ZA, Wanninkhof R, Cai W, Byrne RH, Hu X, Peng T, Huang W (2013) The marine inorganic carbon system along the Gulf of Mexico and Atlantic coasts of the United States: insights from a transregional coastal carbon study. Limnol Oceanogr 58:325–342

Warren DL, Seifert SN (2011) Ecological niche modeling in Maxent: the importance of model complexity and the performance of model selection criteria. Ecol Appl 21: 335–342

Warren DL, Glor RE, Turelli M (2008) Environmental niche equivalency versus conservatism: quantitative approaches to niche evolution. Evolution 62:2868–2883

Warren DL, Glor RE, Turelli M (2010) ENMTools: a toolbox for comparative studies of environmental niche models. Ecography 33:148–158

Weiss AD (2001) Topographic positions and landforms analysis. ESRI Int User Conf, Jul 9–13, San Diego, CA

Wheatley M, Johnson C (2009) Factors limiting our understanding of ecological scale. Ecol Complex 6:150–159

Wheeler AJ, Beyer A, Freiwald A, de Haas H and others (2007) Morphology and environment of cold-water coral carbonate mounds on the NW European margin. Int J Earth Sci 96:37–56

White M, Mohn C, Orren MJ (2007) Physical processes and seamount productivity. In: Pitcher TJ, Morato T, Hart PJB (eds) Seamounts: ecology, fisheries and conservation. Blackwell Publishing, Oxford, p 65–84

White HK, Hsing PY, Cho W, Shank TM and others (2012) Impact of the Deepwater Horizon oil spill on a deep-water coral community in the Gulf of Mexico. Proc Natl Acad Sci USA 109:20303–20308

Wiens JA (1989) Spatial scaling in ecology. Funct Ecol 3: 385–397

Wiens JA, Stralberg D, Jongsomjit D, Howell CA, Snyder MA (2009) Niches, models, and climate change: assessing the assumptions and uncertainties. Proc Natl Acad Sci USA 106:19729–19736

Wiley EO, McNyset KM, Peterson AT, Robins CR, Stewart AM (2003) Niche modeling and geographic range predictions in the marine environment using a machine-learning algorithm. Oceanography (Wash DC) 16: 120–127

Wilson JB (1979) Patch development of the deep-water coral *Lophelia pertusa* (L) on Rockall Bank. J Mar Biol Assoc UK 59:165–177

Wilson MFJ, O'Connell B, Brown C, Guinan JC, Grehan AJ (2007) Multiscale terrain analysis of multibeam bathymetry data for habitat mapping on the continental slope. Mar Geod 30:3–35

Wood JD (1996) The geomorphological characterization of digital elevation models. PhD dissertation, University of Leicester

Editorial responsibility: Paul Snelgrove, St. John's, Newfoundland and Labrador, Canada

Submitted: August 20, 2013; Accepted: April 4, 2014
Proofs received from author(s): June 9, 2014